Ultra small clusters of gold nanoshells detected by SNOM

A. CRICENTI[1], M. LUCE[1], D. MORONI[2], O. SALVETTI[2,3], and M. D'ACUNTO[1,2,3]

[1]Istituto di Struttura della Materia, Consiglio Nazionale delle Ricerche, ISM-CNR, via Fosso del Cavaliere, 100, I–00133, Rome, Italy
[2]Istituto di Scienza e Tecnologie dell'Informazione, Consiglio Nazionale delle Ricerche, ISTI-CNR, via Moruzzi, 1, I-56124, Pisa, Italy
[3]NanoICT laboratory, Area della Ricerca CNR, Pisa, Italy

Metal nanoshells are a type of nanoparticle composed by a dielectric core and a metallic coating. These nanoparticles have stimulated interest due to their remarkable optical properties. In common with metal colloids, they show distinctive absorption peaks at specific wavelengths due to surface plasmon resonance. However, unlike bare metal colloids, the wavelengths at which resonance occurs can be tuned by changing the core radius and coating thickness. One basic application of such property is in medicine, where it is hoped that nanoshells with absorption peaks in the near-infrared can be attached to cancerous tumours. In this paper, we study the changes of optical response in visible and near infrared wavelengths from single to randomly distributed clusters of nanoshells. The results were obtained using a novel formulation of Mie theory in evanescent wave conditions, with a finite-difference time-domain (FDTD) simulation and experimentally on $BaTiO_3$-gold nanoshells using a scanning near-optical microscope. The results show that the optical signal of a randomly distributed cluster of nanoshells can be supplementary tuned with respect to the case of single nanoshell depending by the geometric configuration of the clusters.

1. Introduction

The optical properties of metallic (gold, silver) nanoparticles in the visible and near-infrared (Vis-NIR) domains are governed by the collective response of conduction electrons, the so-called plasmon excitations. These form an electron gas that moves away from its equilibrium position when perturbed by an external light field inducing surface polarization charges that act as a restoring force on the electron gas. The result is a collective oscillatory motion of the electrons characterized by a dominant resonance band that, depending by the shape and size of the gold nanoparticles, falls in the Vis-NIR range [1–2]. Plasmons produce strong effects in both the near- and far-field response of gold nanoparticles. The far-field is fundamental for describing the macroscopic properties of absorption and scattering in colloidal dispersions and metamaterials [3–4]. The near-field properties play the key role for describing the surroundings of the particle within a distance smaller than the order of the light wavelength, the optical properties between nanoparticles, and the interaction with nearby molecules, and sensing powering as in the SERS techniques [5–6]. Since two decades, the near-field is experimentally detected via scanning near-optical microscopy (SNOM) [7]. It is

rather surprising that near-field properties of gold nanoshells can act as nanolens with near-field enhancements that vary from 3 times for gold nanoshells with outer radii of 12–15 nm, until an enhancement factor of ~450 for assemblies of gold nanospheres that can be thought of rows of nanolenses [4]. As a consequence the optical properties of nanoshell clusters play a fundamental role for their usage in a wide range of applications. An example is represented by hyperthermia treatment: the principle for such application is that, when exposed to the appropriate wavelengths of a laser beam, the nanoshells pre-embedded in a tumour absorb energy, then heating up, nevertheless, the healthy tissues along the laser path do not [8–9]. This is because most biological soft tissues have a relatively low light absorption coefficient in the Vis and NIR regions, characteristics known as the tissue optical window. Over such window, NIR light transmits through the tissues with the scattering-limited attenuation and minimal heating preventing the healthy tissues.

The NIR properties of single gold nanoshells (core made of $BaTiO_3$) with dimensions 100–150 nm have been already delineated [10]. In this paper, we place emphasis on the NIR response of ultrasmall nanoshell clusters, aggregates from 2 to 3 nanoshells or 3×3 clusters. The necessity to focus the attention on such ultra small aggregates is based on the

---

*e-mail: davide.moroni@isti.cnr.it

availability of experimental SNOM data recorded in the recent past. The optical responses of such aggregates have been analytically deduced by the reformulation of the Mie theory in evanescent wave regime. In addition, FDTD simulations were addressed to validate the numerical results. In turn, the convolution effect of the SNOM probe tip with the nanoshell clusters was also enlightened.

2. Evanescent-wave theory of gold nanoshells

A fundamental solution describing electromagnetic wave scattering by a spherical particle was found in 1908 by Gustav Mie [11]. With the advent of near-field optics and plasmonics, evanescent electromagnetic waves have attracted enormous interest, both for theory and applications, in a special way, in systems made of nanoscale particles [12–13].

In this section, we briefly describe the modified Mie theory in near-field conditions, for single- or cluster nanoparticles, analogous to single-cluster nanoshells. In turn, the effects of the SNOM tip with particles and subsequent modifications to the optical cross sections are discussed.

The starting point of a Mie modified theory are the expressions for the optical cross-sections of a single particle in evanescent wave approach [14–17]. For a spherical particle of gold with radius $a<<\lambda$, the extinction and scattering cross sections for s-polarized and p-polarized incident light are respectively

$$\sigma_{ext}^{s} = \frac{2\pi}{\eta k^{2}} \text{Re} \sum_{n=1}^{\infty} (2n+1)(a_{n}\Pi_{n} + b_{n}T_{n}), \quad (1a)$$

$$\sigma_{sca}^{s} = \frac{2\pi}{\eta k^{2}} \text{Re} \sum_{n=1}^{\infty} (2n+1)(|a_{n}|^{2}\Pi_{n} + |b_{n}|^{2}T_{n}), \quad (1b)$$

$$\sigma_{ext}^{s} = \frac{2\pi}{\eta k^{2}} \text{Re} \sum_{n=1}^{\infty} (2n+1)(a_{n}T_{n} + b_{n}\Pi_{n}), \quad (1c)$$

$$\sigma_{sca}^{s} = \frac{2\pi}{\eta k^{2}} \text{Re} \sum_{n=1}^{\infty} (2n+1)(|a_{n}|^{2}T_{n} + |b_{n}|^{2}\Pi_{n}), \quad (1d)$$

where the coefficients a_n and b_n are the scattering coefficients of the *TM*-modes and *TE*-modes of the spherical particles, Π_n and T_n are respectively defined as

$$\Pi_{n}(\theta_{k}) = \frac{2}{n(n+1)} \sum_{m=-n}^{n} \frac{(n-m)!}{(n+m)!} \left| m \frac{P_{nm}(\cos\theta_{k})}{\sin\theta_{k}} \right|^{2}, \quad (2a)$$

$$T_{n}(\theta_{k}) = \frac{2}{n(n+1)} \sum_{m=-n}^{n} \frac{(n-m)!}{(n+m)!} \left| m \frac{dP_{nm}(\cos\theta_{k})}{d\theta_{k}} \right|^{2}, \quad (2b)$$

where θ_k is the angle of incidence in the reference frame of the particle and it is quantified by the Snell's law on the incidence angle at the interface substrate-medium (air)

$$\sin\theta_{k} = \frac{n_{S}}{n_{M}} \sin\theta_{i}, \quad (3)$$

with n_S being the index of refraction of the substrate and n_M the index of refraction of the surrounding medium (in our case the air), and P_{nm} are the associated Legendre polynomials. In Eqs. (1a)–(1d), the normalization factor η assumes the expression:

$$\eta = \frac{n_{S}}{n_{M}} \sin\theta_{i} \left(1 + \sum_{m=1}^{\infty} \frac{(\kappa a)^{2m}}{m!(m+1)!} \right), \quad (4)$$

with $\kappa = 2\pi / \lambda \sqrt{(n_{S}^{2}\sin\theta_{i} - n_{M}^{2})}$. In Eqs. (1a)–(1d), the polarizations dependence of the cross sections is due to the fact that p- and s- polarised evanescent waves are not related to each other by a simple rotation. The most important consequence of the Eqs. (1a) – (1d) as proposed by Quinten *et al.* is that they are valid also for nanoshells [14]. Only the expressions for the coefficients a_n and b_n differ in these cases. Here, we wish to consider the equivalent formulation of the equations (1.a–d) to the case of a cluster aggregate of N nanoparticles, in this case, the extinction and scattering cross sections are given by Ref. 15

$$\sigma_{ext}(N) = \frac{2\pi}{k^{2}} \sum_{i=1}^{N} \sum_{n=1}^{\infty} \sum_{m=-n}^{n} \text{Re}\{\alpha_{nm}(i) + \beta_{nm}(i)\}, \quad (5a)$$

$$\sigma_{sca}(N) = \frac{2\pi}{k^{2}} \sum_{i=1}^{N} \sum_{n=1}^{\infty} \sum_{m=-n}^{n} |\alpha_{nm}(i)|^{2} + |\beta_{nm}(i)|^{2} +$$
$$+ \frac{2\pi}{k^{2}} \sum_{i=1}^{N} \sum_{n=1}^{\infty} \sum_{m=-n}^{n} \text{Re}\left\{ \alpha_{nm}^{*}(i)\left[1 - \frac{\alpha_{nm}(i)}{a_{n}(i)}\right] + \beta_{nm}^{*}(i)\left[1 - \frac{\beta_{nm}(i)}{b_{n}(i)}\right] \right\}$$
$$(5b)$$

where $\alpha_{nm}(i)$ and $\beta_{nm}(i)$ are the expansion coefficients of the scattered wave from the particle i. Such coefficients can be found resolving solutions of linear sets of equations following from Maxwell's equations with boundary conditions at the surface of each particle i. Generally, the electromagnetic coupling becomes negligible for centre-to-centre distances $d\sim10a$, where a is the radius of the nanoshells, then the cross sections of the aggregate reduce to the sum over cross sections of N isolated spheres.

Extinction and scattering of light by an arbitrary N-spherical nanoshell cluster as given by Eqs. (5a)–(5b) will be calculated in the next section.

3. Optical response from single to randomly distributed clusters of gold shell nanoparticles: numerical and simulated results

Absorption and scattering of light by an arbitrary N-spherical nanoshell cluster depend on the sizes of the primary nanoshell, the size and topology of the cluster, the particles' materials and the polarization and propagation direction of the incident wave. The simplest aggregate is a pair of nanoshells. In this case, two principal excitation modes of the aggregate are obtained: the longitudinal mode, when the

A. Cricenti

electric field vector of the incident wave is along with the axis of the pair, and transverse mode with the electric field being perpendicular to this axis. In the general case of arbitrary incidence of the plane wave both modes contribute to a certain amount to the absorption and scattering by the pair. In the case of a three nanoshell cluster (triplet aggregate), the situation is very close to pair particles when the three particles are located along a line (linear triplet cluster), like in Fig. 1. In the case of triplet aggregates, planes waves *p*-polarized, characterized by the transversal oscillation of the electric field, produce the most relevant plasmon oscillation between the nanoshells, with the appearance of supplemental modes due to the geometry of the cluster. For higher and complex clusters extinction and scattering responses become more complicated, so we will focus the attention on the difference between a single nanoshell and a linear triplet cluster.
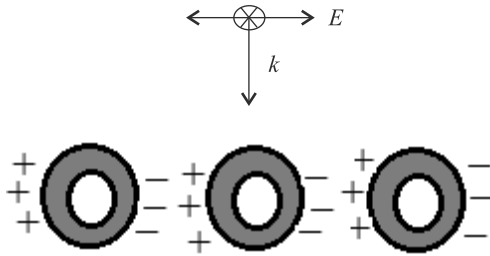
Fig. 1. A linear triplet cluster of nanoshells perpendicular to wave vector with *p*-polarized and *s*-polarized electric field vector (perpendicular to the plane wave and denoted by the cross symbol). Since the *p*-polarization presents an electric field oscillating along the axis of the cluster (longitudinal mode), the plasmonic effect is amplified and supplemental modes due to the interaction between subsequent nanoshells can be observed.

The optical properties of nanoshell clusters obtained using the extended Mie theory in near-field conditions, can be described in terms of normalized efficiencies for the extinction, scattering and absorption cross sections divided by the geometrical cross section of the clusters. The cross sections as given by Eqs (5a)–(5b) integrating Eqs. (1a)–(1d) are calculated on the basis of the generalized multiparticle Mie approach [17]. The environment medium is the air. The incident radiation can be *p*-polarized or *s*-polarized and its wave vector is directed perpendicularly to the nanoparticle array plane as in Fig. 1. For sufficiently small particles, the relation $T_n > \Pi_n$ leads to $\sigma_{sca}^p > \sigma_{sca}^s$ for all wavelengths, and the absolute value of the Mie coefficients a_n for electric multipoles are larger than the coefficients b_n for the magnetic multipoles to each order n. The absorption efficiency of the numerical integration of Eqs (5a)–(5b) for a single nanoshell and a triplet or a 3×3 nanoshell clusters using the generalized multiparticle Mie approach in evanescent wave conditions are summarized in Fig. 2. Absorption efficiency is also the prevalent optical mechanism for particle with a varying gold layer in the range 0–100 nm, with a BaTiO₃ core dimension fixed of 100 nm [18–19].
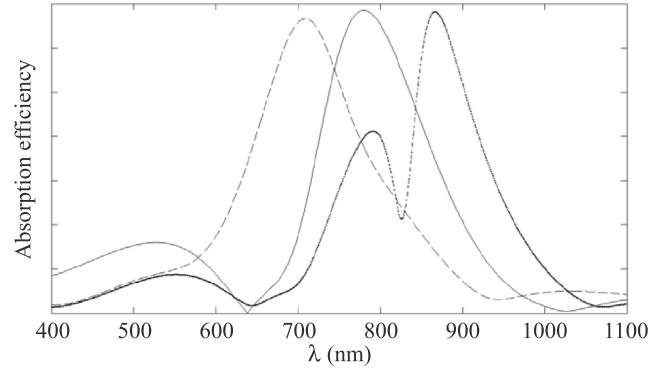
Fig. 2. Absorption efficiency spectra as a function of external e.m. wavelength for, respectively, an isolated BaTiO$_3$-gold (80 nm – 40 nm) nanoshell, dashed line, for a triplet aggregate for the same nanoshell composition, continuous line, and 3×3 nanoshell cluster, dot-dashed line.

A FDTD simulation model is applied to analyze the near-field properties around the irradiated nanoparticles. This computational technique is commonly recognized to give an adequate picture of the electromagnetic field distribution in the near and far-fields around structures with arbitrary shapes. The main signal observed in the FDTD simulation is the Poynting vector of the evanescent wave. Since the Poynting vector is also the collected signal by the SNOM, the FDTD simulation gives results that can be immediately compared with the experimental results. However, the observed intensity collected by the SNOM aperture tip needs a comment. As I_{inc} we choose the incident intensity, averaged over the cross-sectional area of the SNOM aperture tip perpendicular to the Poynting vector ($S = E \times H$) of the evanescent wave, then we have

$$I = \frac{1}{\pi a^2} \iint \langle S_{inc} \rangle n dA = I_{inc} \exp(-2\kappa d) \frac{I_1(2\kappa a)}{\kappa a} \frac{n_S}{n_M} \sin \theta_i,$$

(6)

where $I_l(2\kappa a)$ is the modified Bessel function of first order with argument $2ka$, and the normalization factor

$$\eta = \frac{I_1(2\kappa a)}{\kappa a} \frac{n_S}{n_M} \sin \theta_i$$

(7)

is the analogous as Eq. (4). In Eq. (6), d is the *z*-height of the evanescent wave before the complete extinction; in the FDTD simulation we tested the Poynting vector for *z* in the 10–30 nm range. See Fig. 3.

To exhibit the relative absorption and scattering ability of the nanoshells, the cross sections for absorption and scattering can be defined as $\sigma_{abs} = W_{abs}/I_{inc}$ and $\sigma_{scat} = W_{scat}/I_{inc}$, respectively, while the efficiencies are defined as $Q_{abs} = \sigma_{abs}/A$ and $Q_{scat} = \sigma_{scat}/A$, for the absorption and the scattering processes, respectively. Here, the $I_{inc} = (1/2)\varepsilon_0 c E^2$ represents the intensity of the incident wave, $A = \pi r^2$ is the particle cross-section are projected onto a plane perpendicular to the incident wave, and *r* is the total radius on the nano-
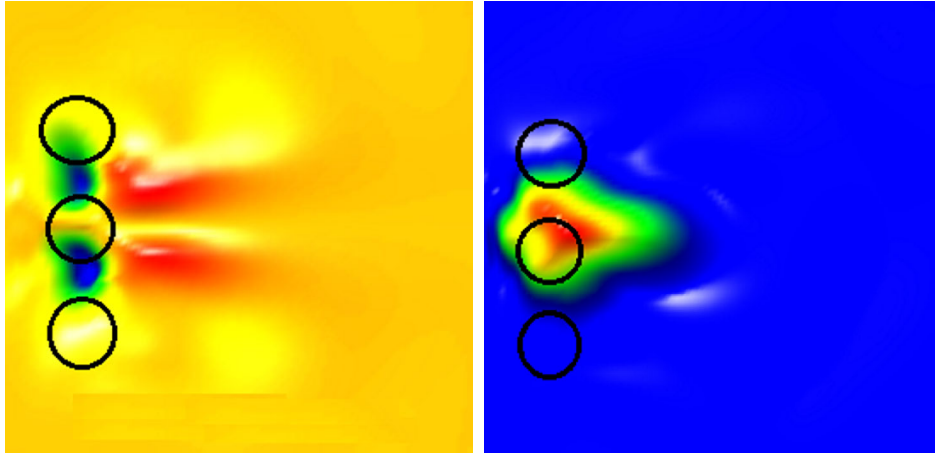
Fig. 3. FDTD plots of the scattered intensity (Poynting vector) from a triplet cluster for two different wavelengths, λ = 632 nm (left), and λ = 795 nm, right, as observed at z = 20 nm from the particle surface.

sphere. Finally, the absorption and scattering energy $W_{abs/scat}$ are defined respectively as

$$W_{abs} = \frac{1}{2} \mathrm{Re}\left[\int\int (\mathbf{E}_{tot} \times \mathbf{H}^*_{tot})\mathbf{n}ds \right]$$

$$\text{and} \quad W_{scat} = \frac{1}{2} \mathrm{Re}\left[\int\int (\mathbf{E}_{scat} \times \mathbf{H}^*_{scat})\mathbf{n}ds \right]. \quad (8)$$

In far field we can insert the components fields as given by Eqs. (5a)–(5b), inside Eq. (8), and integrating on all a solid angle; on the contrary, in near field, if we consider a finite dimension of tip aperture, we have that the scattered and absorbed intensity being proportional to the solid angle.

In addition, if we consider a near field solution of electric and magnetic fields and the field enhancement in z-direction in proximity of the SNOM probe tip, under some specific conditions we can observe intense enhanced absorption being meanly the E_z components under the SNOM tip about 10 times larger compared to the in-plane components, it is reasonable to suppose that when the probe signal displays a point-like absorption peaks, this can be identified with a nanoshell [20]. This is because the field enhancement caused by the local surface plasmon resonance mainly focuses on the metal-dielectric interface (and decays exponentially); in addition it is not absorbed by the biological tissue due to the transparency window.

4. Experimental results

The extinction signals of small clusters of nanoshells seed on SiO_2 substrates in air were measured making use of a home-made SNOM operating in air in collection mode with different illumination wavelengths ranging from visible to near infrared.

The SNOM used for the reflection mode measurements is composed by two separable cylindrical supports: the lower one contains the sample holder mounted on top of a piezoelectric scanner which is embedded in a motor controlled x-y-z stage. A piezo-modulated stretched optical fi-

bre with a few tens of a nanometer pinhole and a shear-force apparatus mounted inside the top cylinder allow for topographic measurements. In Fig. 4, a schematic sketch of the experimental setup is shown. Any additional information on the home-made SNOM can be found in Ref. 21. Home--made procedure for tip manufacturing was based on chemical etching process producing tips with aperture of nearly 50 nm diameter. After etching process, the tip are coated by a tiny metallic (evaporated aluminium) layer so as to prevent light from coupling into the fibre from anywhere other than at the aperture of the probe.

The sample to be measured consisted of nanoshells composed by a core of $BaTiO_3$ (80–100 nm) and a gold shell varying in a 20–40 nm range. The nanoshells were seeded on a SiO_2 surface, Fig. 5. The extinction signal of the samples has been detected in a reflection acquisition mode: the sample can be illuminated on top by an external source, laser, with different wavelengths λ, (λ = 488 nm, 632 nm, 780 nm were used), in turn, an optical fibre was used for the detection of the reflected signals. The results obtained using the SNOM in collection mode with a 780 nm wavelength laser light have been already described elsewhere [20]. The absorption sources were meanly of two types, point-like and enlarged. Point-
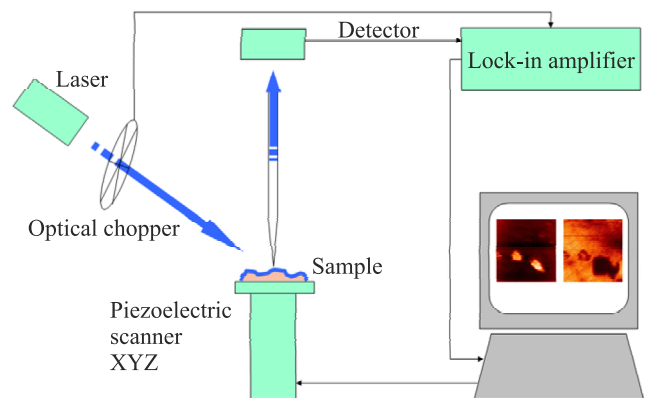

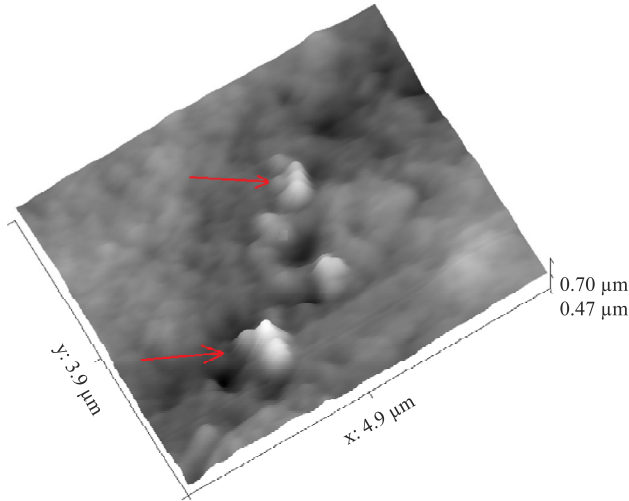Fig. 4. Schematic sketch of the experimental setup used for the SNOM acquisitions.

Fig. 5. Topographic image of a silicon substrate with small clusters of gold nanoshells as indicated by the red arrows.

-like absorption presents dimension very close to nanoshells falling in the range 120–150 nm diameters, so that the identification of such points with the gold nanoparticles is immediate. Here, we wish to focus the attention on the nanoshell clusters, in fact, enlarged absorption regions could be associated to nanoparticles clustering, Fig. 5.

The isolated point-like sources can be immediately identified as the core-shell nanoparticles. Nevertheless, the larger absorption zones as shown in Fig. 2 could be identified

as clusters of particles creating an effect of interference between nanoparticles close one each other. The explanation of this consideration can be described as follows.

The near-field radiation of a particle located at *a* and collected at SNOM tip aperture is approximately given by the expression [22]

$$E_z(\mathbf{r}, t) \cong E_0(\mathbf{p} \cdot \mathbf{n})(\mathbf{n} \cdot \mathbf{e}_a) \frac{\cos(kr_a - \omega t)}{\sqrt{r_a}} \exp(-r_a/l), \quad (9)$$

where E_0 and $\mathbf{p}$ are the electric field amplitude and the polarization direction of the illuminating light, respectively; $r_a = |\mathbf{r}_a| = |\mathbf{r} - \mathbf{a}|$ is the magnitude of the separation vector with $\mathbf{e}_a = \mathbf{r}_d/r_a$ being the unit vector. The terms $\mathbf{p} \cdot \mathbf{n}$ and $\mathbf{n} \cdot \mathbf{e}_a$ describe the role of the polarization on the efficiency of near field plasmon-e.m. coupled excitation, being the $\mathbf{n}$ the normal vector to the probe (recognized as the maximum dipole radiation) and the cosine angular distribution of the radiation, respectively. The two factors k and l represent the propagation constant and the length of the nanoparticles plasmonic field, respectively. The detected SNOM signal is formed by the complex light scattering processes between the tip and the sample, mixing different field components. Thus, electromagnetic field collected near the probe cannot be simply linked to a specific component of the unperturbed electromagnetic field distribution.

The different dimensions of the absorption in Fig. 6 can be described with a mechanical model consisting of three
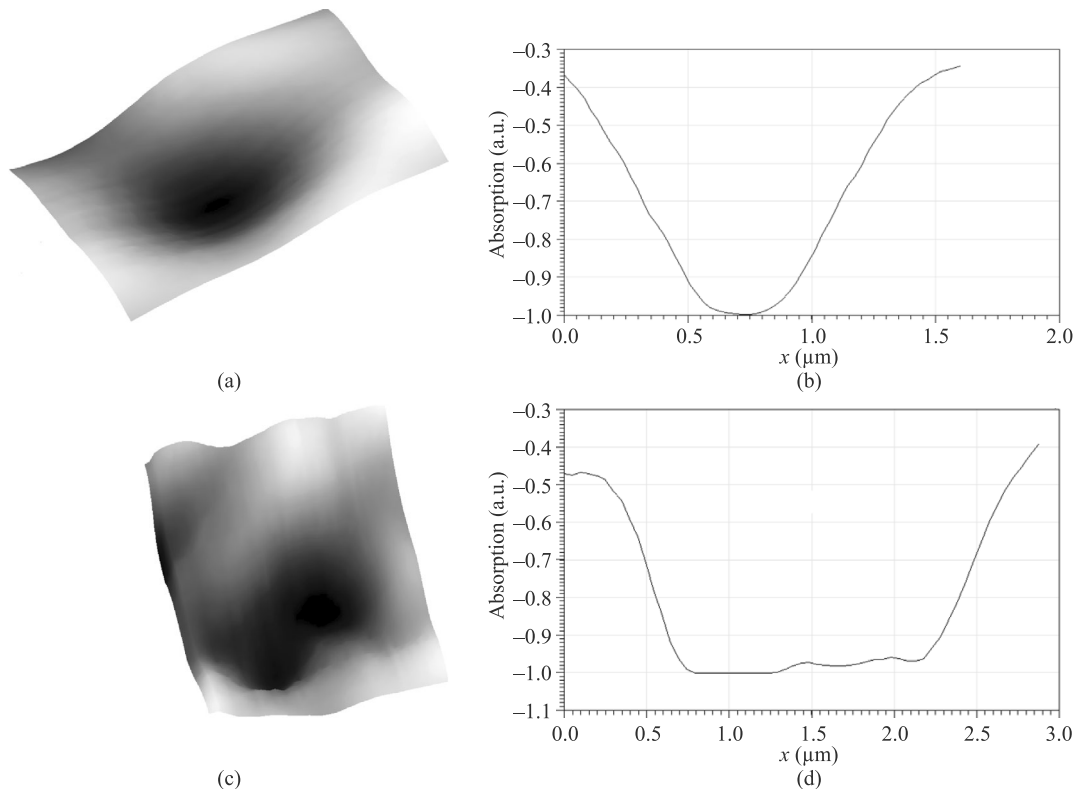

Fig. 6. Effects of the convolution between the nanoshells with the metallic tip: (a)–(b), optical response of a single gold nanoshell and correspondent profile, respectively; (c)–(d), the same as in (a)–(b), but for a cluster of three nanoshells as indicated by the red arrows in Fig. 5. The spatial dimension of the absorption of the triplet aggregate cluster is significantly higher than in the case of a single nanoshell.
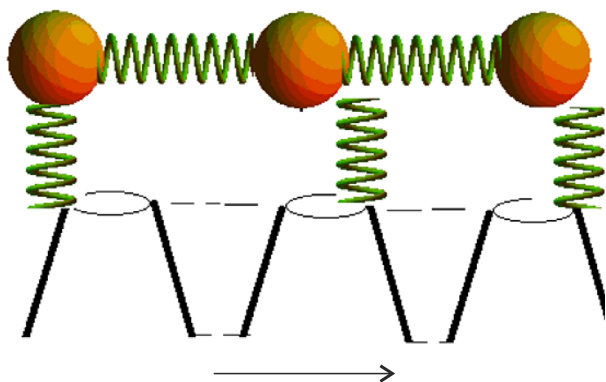
Fig. 7. Schematic sketch of the absorption enlargement due to the interaction between SNOM tip and gold clusters: the absorption power of the cluster of gold nanoshells can be pictured as a three oscillator's model, where the oscillators are connected with springs one each other. When the metallic SNOM probe tip slides very close to the particles, a dynamical supplemental interaction depicted by a new spring is created and destroyed as the tip passes along the cluster.

coupled oscillators [23]. The plasmon modes are modelled as three interacting oscillators of frequencies ω_1, ω_2 and ω_3, and the three oscillators interact with three springs like in Fig. 7. When the SNOM probe metallic tip is scanning the sample in proximity of the gold nanoshell within a distance falling in the height of the evanescent wave, then the three oscillators system couples with the metallic tip with a spring that appears and disappears as the tip moves towards to, Fig. 7. The result is a system that changes the strength of the absorbed power by the gold nanoshells, coupled to possible red shift and the rise of possible multimode response. The measurable effect in our system is the observation of a large domain of absorption, due to the convolution of the gold nanoshell with the probe tip.

The results represented in Figs. 2, 3 and 6 indicate that ultra-small nanoshell clusters with dimensions 100–150 nm offer great advantages due to their absorption response in the NIR range. Other than already known optical tunability, small aggregates of such nanoshells present a new effect, i.e., the growth of the region of absorption due to the interaction with the SNOM probe tip. This in an effect not observed in the case of a single nanoshell.

5. Conclusive Remarks

Metal nanoshells are a type of nanoparticle composed by a dielectric core and a metallic coating. They show distinctive absorption peaks at specific wavelengths due to a surface plasmon resonance with the basic advantage that the wavelengths at which resonance occurs can be tuned by changing the core radius and coating thickness. In this paper, we have studied the changes of optical response in visible and near infrared wavelengths from single to randomly distributed ultra-small clusters of nanoshells. We have presented experimental results on the extinction, absorption

and scattering cross sections of BaTiO$_3$-gold nanoshells (100–150 nm) using a scanning near-optical microscope in reflection mode. The results were compared with a numerical approach based on a formulation of Mie theory in evanescent wave conditions and with a FDTD simulation. The results show that the optical signal of a randomly distributed cluster of nanoshells can be supplementary tuned with respect to the case of single nanoshell depending by the geometric configuration of the clusters.

Acknowledgements

References

1. S. Maier, *Plasmonics: Fundamentals and Applications*, Springer, (2007).
2. A.V. Zayats, I.I. Smolyaninov, and A.A. Maradudin, *Phys. Rep.* **408**, 131–31, (2005).
3. K.L. Kelly, E. Coronado, L.L. Zhao, and G.C. Schatz, *J. Phys. Chem.* **B107**, 668 (2003).
4. Z. Li, S. Butun, and K. Aydin, *ACS Photonics* **1**, 228–234, 2014.
5. S. Schlucker, *Surface Enhanced Raman Spectroscopy: Analytical, Biophysical and Life Science Applications*, Wiley, 2010.
6. M. Baia, S. Astilean, and T. Iliescu, *Raman and SERS Investigations of Pharmaceuticals*, Springer-Verlag, Berlin, 2008.
7. www.pyat.com.tw/upload/20130327005533.pdf
8. C. Liu, C.C. Mi, and B.Q. Li, *IEEE T. Nanobioscience* **7**, 206–214, 2008.
9. T.A. Erickson and J.W. Tunnell, in *Nanomaterials for the Life Science* ,Vol. 3: *Mixed Metal Nanomaterials*, C.S.S.R. Kumar, Wiley 2009.
10. M. D'Acunto, D. Moroni, and O. Salvetti, "Nanoscale biomolecular detection limit for gold nanoparticles based on near-infrared response", *Advances in Optical Technologies*, (2012).
11. G. Mie, "Articles on the optical characteristics of turbid tubes, especially colloidal metal solutions", *Ann. Phys.* **25**, 377 (1908).
12. V. Myroshnychenko, J. Rodríguez-Fernández, I. Pastoriza-Santos, A.M Funston, C. Novo, P. Mulvaney, L.M. Liz-Marzán, F.J, García de Abajo, „Modelling the optical response of gold nanoparticles", *Chem. Soc. Rev.* **37.9**, 1792–1805 (2008). S.V. Boriskina, *Plamsonics* **15**, 431–461 (2010).
13. R. Wannemache, M. Quinten, and A. Pack, "Evanescent-wave scattering in near-field optical microscopy", *J. Microsc.* **194.2–3**, 260–264(1999).
14. M. Quinten, A. Pack, and R. Wannemacher, "Scattering and extinction of evanescent waves by small particles", *Appl. Phys. B: Laser Opt.* **68.1**, 87–92 (1999).
15. M. Quinten, "Evanescent wave scattering by aggregates of clusters–application to optical near-field microscopy", *Appl. Phys.* **B70.4**, 579–586 (2000).

16. A.Y. Bekshaev, K.Y. Bliokh, and F. Nori, "Mie scattering and optical forces from evanescent fields: A complex-angle approach", *Opt. exp.* **21.6**, 7082–7095 (2013).

17. N.N. Nedyalkov, A.Og. Dikovska, I.G. Dimitrov, R.G. Nikov, P.A. Atanasov, and R.A. Toshkova, "Far-and near--field optical properties of gold nanoparticle ensembles", *Quantum Electron+* **42.12**, 1123 (2012).

18. Ch.M. Dutta, T.A. Ali, D.W. Brandl, T.-H. Park, and P. Nordlander, "Plasmonic properties of a metallic torus", *J. Chem. Phys.* **129**, 084706 (2008).

19. M. D'Acunto, A. Cricenti, and M. Luce, submitted to Nanospectroscopy.

20. A. Cricenti, V. Marocchi, R. Generosi, M. Luce, P. Perfetti, D. Vobornik, G. Margaritondo, D. Talley, P. Thielen, J.S. Sanghera, I.D. Aggarwal, J.K. Miller, N.H. Tolk, and D.W. Piston, "Optical nanospectroscopy study of ion-implanted silicon and biological growth medium", *J. Alloy. Comp.* **362**, 21–25 (2004).

21. P. Dvořák, T. Neuman, L. Břínek, T. Šamořil, R. Kalousek, P. Dub, P. Varga, and T. Šikola, "Control and near-field detection of surface plasmon interference patterns", *Nano Lett.* **13**, 2558–2563 (2013).

22. S. Mukherjee, H. Sobhani, J. Britt Lassiter, R. Bardhan, P. Nordlander, and N.J. Halas, "Fanoshells: nanoparticles with built-in Fano resonances", *Nano Lett.* **10**, 2694–2701 (2010).

23. J. Zuloaga, and P. Nordlander, "On the energy shift between near-field and far-field peak intensities in localized plasmon systems", *Nano Lett.* **11**, 1280–1283 (2011).